International Journal of Precision Engineering and Manufacturing Vol. 5, No. 4, October 2004.

Nonlinear Dynamic Analysis of a Large Deformable Beam Using Absolute Nodal Coordinates

Jong-Hwi Seo[1,#], Il-Ho Jung[1], Tae-Won Park[2]

[1] Graduate School of Mechanical Engineering, Ajou University, Suwon, South Korea
[2] Division of Mechanical Engineering, Ajou University

ABSTRACT

A very flexible beam can be used to model various types of continuous mechanical parts such as cables and wires. In this paper, the dynamic properties of a very flexible beam, included in a multibody system, are analyzed using absolute nodal coordinates formulation, which is based on finite element procedures, and the general continuum mechanics theory to represent the elastic forces. In order to consider the dynamic interaction between a continuous large deformable beam and a rigid multibody system, a combined system equations of motion is derived by adopting absolute nodal coordinates and rigid body coordinates. Using the derived system equation, a computation method for the dynamic stress during flexible multibody simulation is presented based on Euler-Bernoulli beam theory, and its reliability is verified by a commercial program NASTRAN. This method is signinficant in that the structural and multibody dynamics models can be unified into one numerical system. In addition, to analyze a multibody system including a very flexible beam, formulations for the sliding joint between a very deformable beam and a rigid body are derived using a non-generalized coordinate, which has no inertia or forces associated with it. In particular, a very flexible catenary cable on which a multibody system moves along its length is presented as a numerical example.

Key Words : Large Deformable Beam , Multibody Dynamics, Absolute Nodal Coordinates, Dynamic Stress, Sliding Joint, Flexible Catenary Cable.

1. Introduction

A very flexible beam can be used to model various types of engineering parts such as cables, wires, and ropes. The dynamic properties of the flexible beam in such parts can be very important factors in influencing the dynamic stability and behavior of a mechanical multibody system that interacts with the beam.

There have been many studies on the mechanical properties of beams [1], but most have been restricted to structure-based problems such as those associated with railroad, bridge, and building design. In other words, there is still an insufficient number of studies that simultaneously analyze multibody systems and their dynamic interaction with a nonlinear large deformable beam. This is because dynamic analysis becomes very complex when it is coupled with a multibody system.

In studies that analyze the dynamic problems of a flexible beam with which a mass or a multibody system interacts, a lumped mass is considered where the continuous beam is modeled as discrete [2-4]. This method has been mainly used for the modeling of very flexible continuous mechanics, such as belts, chains, and cables in the multibody dynamic analysis method, but a large number of lumped mass needs to be used. So the numerical efficiency may decline. Moreover, it is very difficult to define the sliding or interconnecting constraints between a multibody system and a continuous flexible beam.

To analyze flexible multibody dynamics using modal coordinates, Hwang [5] derived a constraint equation for a

☞ Manuscript received: January 8, 2004 ;
Accepted: June 14, 2004
Corresponding Author:
Email: jonghwi@empal.com
Tel: +82-31-219-2952, Fax: +82-31-219-1965

sliding joint that can move along a flexible body. However, the boundary condition changes depending on the relative motion of the two flexible bodies connected by the joint, so it is hard to present the exact constraint condition of the sliding joint by using a deformation mode that depends on time. In addition, the method assumed linear elastic deformation, so it is hard to apply to the dynamic problems of a large deformable beam.

Park [6] derived the combined differential-algebraic equations of motion using a multibody dynamics theory to analyze a constrained multibody mechanical system moving on an elastic beam structure with a contact effect. This method can consider various foundation supports and constraints, as well as the structural damping effect of the beam structure. However, this method assumed linear elastic deformation, so it is difficult to apply to large deformable beam problems.

Sugiyama [7] proposed a constraint equation for a sliding joint wherein a mass moves along a large deformable beam using absolute nodal coordinates formultion. This method can analyze the dynamic interaction between the cable and the mass by assuming the large deformable cable as a beam element, but when the cable is modeled as more than two finite beam elements, it is hard to define the sliding joint due to discontinuousness at the nodal point.

Simo and Vu-Quoc [8] proposed a large rotation vector formulation to analyze a very flexible beam, included in a multibody system. But this formulation leads to a redundant representation and can lead to fundamental problems in defining the generalized forces associated with the beam generalized coordinates. In other words, this can lead to singularity problems when a slender beam is considered.

In addition to these studies, there have also been studies that analyzed the dynamic behavior and vibration of a beam [9-12], but most of them only calculated dynamic properties from the viewpoint of structural dynamics. Thus, studies on the dynamic problems of a flexible beam coupled with a multibody system are rare.

In this paper, to consider the dynamic interaction between a continuous large deformable beam—which can be modeled as a cable or a wire—and a rigid multibody system, a generalized system equations of motion is derived using absolute nodal coordinates [13-14] and rigid body coordinates. A very flexible catenary cable on which a multibody system moves along its length is presented as a numerical example in this paper. To do this, formulations for the sliding joint between a very flexible beam and a rigid body were derived using a non-generalized coordinate, which has no inertia or forces. This sliding joint is very important to many mechanical applications such as ski lifts, cable cars, the pantograph-catenary of high-speed trains, and pulley systems.

In addition, a method for calculating the dynamic stress of a large deformable beam in flexible multibody dynamics using absolute nodal coordinates is presented and is compared with the results from the commercial analysis program NASTRAN [15]. The calculated dynamic stress can be used to predict the fatigue life of a mechanical part [16]. In other words, the presented method of this paper is significant in that the structural and multibody dynamics models can be unified into one numerical system.

In this study, the multibody system was considered to be rigid bodies, and the large flexible beam was modeled using the absolute nodal coordinates in order to present the geometric nonlinearity and large deformation phenomena. The study was conducted focusing on the 2-dimensional system.

2. Dynamic Equations of a Large Deformable Beam Using Absolute Nodal Coordinates

2.1 Introduction of Absolute Nodal Coordinates Formulation

Fig. 1 shows the global displacement and slope of absolute nodal points at both ends of the 2-dimensional beam element i for the global reference frame, which can present the large deformable property of a cable or a wire

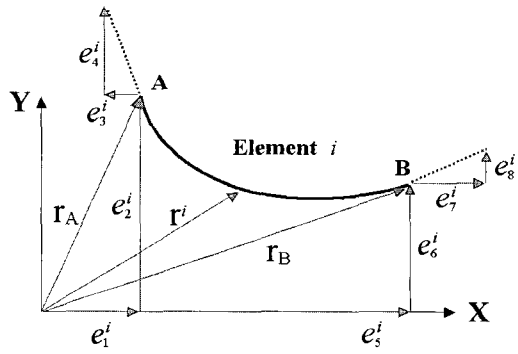

Fig. 1 The global position of a point on a beam element i

Eq. (1) shows that an arbitrary displacement of the beam element can be expressed with the shape function and absolute nodal coordinates.

$$\mathbf{r}^i = \begin{bmatrix} r_x^i \\ r_y^i \end{bmatrix} = \mathbf{S}^i(x)\ \mathbf{e}^i(t) \tag{1}$$

Here, $\mathbf{r}^i$ is an arbitrary point in the beam element for the global reference frame and $\mathbf{S}^i$ is the shape function of the element. The shape function can be expressed using the cubic polynomial equation on the deformation in longitudinal and transversal directions as in Eq.(2). The shape function of the equation is defined not in local nodal coordinates but in a global reference frame.

$$\mathbf{S}^i(x) = \begin{bmatrix} S_x^i \\ S_y^i \end{bmatrix} = \begin{bmatrix} S_1 & 0 & S_2 & 0 & S_3 & 0 & S_4 & 0 \\ 0 & S_1 & 0 & S_2 & 0 & S_3 & 0 & S_4 \end{bmatrix}$$
$$S_1 = 1 - \frac{3x^2}{l^2} + \frac{2x^3}{l^3},\quad S_2 = x - \frac{2x^2}{l} + \frac{x^3}{l^2} \tag{2}$$
$$S_3 = \frac{3x^2}{l^2} - \frac{2x^3}{l^3},\quad S_4 = -\frac{x^2}{l} + \frac{x^3}{l^2}$$

Here, l is the length of the beam element i before the deformation, and x is the an arbitrary displacement in longitudinal direction. $\mathbf{e}^i$ is the absolute nodal coordinates vector that shows the displacement and slope of the nodal points at two ends of the element, and it can be written as the following equation.

$$\mathbf{e}^i = [e_1^i\ e_2^i\ e_3^i\ e_4^i\ e_5^i\ e_6^i\ e_7^i\ e_8^i]^T \tag{3}$$

Here, e_1^i, e_2^i, e_5^i, e_6^i is the absolute nodal displacement of nodal points A and B, and e_3^i, e_4^i, e_7^i, e_8^i is the global slope. These can be written as Eq. (4).

$$\left.\begin{aligned} e_1^i &= r_x^i(x=0)\ ,\ e_2^i = r_y^i(x=0) \\ e_3^i &= \frac{\partial r_x^i(x=0)}{\partial x},\ e_4^i = \frac{\partial r_y^i(x=0)}{\partial x} \\ e_5^i &= r_x^i(x=l)\ ,\ e_6^i = r_y^i(x=l) \\ e_7^i &= \frac{\partial r_x^i(x=l)}{\partial x},\ e_8^i = \frac{\partial r_y^i(x=l)}{\partial x} \end{aligned}\right\} \tag{4}$$

Using these displacement kinematics, the kinetic energy of the beam element i can be calculated as Eq. (5) with Eq. (1).

$$\begin{aligned} T^i &= \frac{1}{2}\int_{V^i} \rho^i\, \dot{\mathbf{r}}^{i\,T}\, \dot{\mathbf{r}}^i\, dV^i \\ &= \frac{1}{2}\dot{\mathbf{e}}^{i\,T}\left(\int_{V^i} \rho^i\, \mathbf{S}^{i\,T}\, \mathbf{S}^i\, dV^i\right)\dot{\mathbf{e}}^i \\ &= \frac{1}{2}\dot{\mathbf{e}}^{i\,T}\, \mathbf{M}^i\, \dot{\mathbf{e}}^i \end{aligned} \tag{5}$$

Here, ρ^i and V^i are the density and volume of the beam element i. $\mathbf{M}^i$ is the mass matrix, and it has properties of a symmetric matrix. It can only be defined by $\mathbf{S}^i$, so if the system is determined, it only needs to be calculated once. Since it is a function of length l and mass m, it can be rewritten as Eq. (6).

$$\mathbf{M}^i = \int_{V^i} \rho^i \mathbf{S}^{i\,T}\, \mathbf{S}^i dV^i = m^i \int_0^l \mathbf{S}^{i\,T}\, \mathbf{S}^i dx \tag{6}$$

The elastic force generated from the deformation in longitudinal and transverse direction of the beam element can be obtained after calculating the total strain energy and partially differentiating the result on the generalized coordinates. The study obtains the elastic force based on the classic Euler-Bernoulli beam theory.

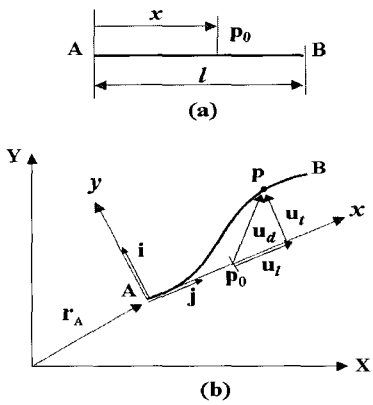

Fig. 2 (a) Original and (b) Current deformation of longitudinal and transverse

Fig. 2 shows the deformation of longitudinal direction and transversal direction, and the strain at the arbitrary point $\mathbf{P_0}$ can be calculated using Eq. (7).

$$\mathbf{u} = \begin{bmatrix} u_x \\ u_y \end{bmatrix} = \mathbf{r}_p - \mathbf{r}_A = (\mathbf{S}^i - \mathbf{S}^i{}_A)\,\mathbf{e}^i$$
$$\mathbf{u}_d = \begin{bmatrix} u_l \\ u_t \end{bmatrix} = \begin{bmatrix} \mathbf{u}^T\mathbf{i} - x \\ \mathbf{u}^T\mathbf{j} \end{bmatrix} = \begin{bmatrix} u_x i_x + u_y i_y - x \\ u_x j_x + u_y j_y \end{bmatrix} \tag{7}$$

Here, $\mathbf{S}^i{}_A$ is equal to $\mathbf{S}^i\big|_{x=0}$. $\mathbf{i}$ and $\mathbf{j}$ are the unit vectors of the x-axis and y-axis of the beam's reference coordinates. The total strain energy of the beam can be obtained by integrating the strain energy generated from the arbitrary displacement in the total length, as in Eq. (8) [17].

$$U^i = \frac{1}{2}\int_0^l \left(Ea\left(\frac{\partial u_l}{\partial x}\right)^2 + EI\left(\frac{\partial^2 u_t}{\partial x^2}\right)^2 \right) dx = \frac{1}{2}\mathbf{e}^{iT}\mathbf{K}_a^i\mathbf{e}^i \tag{8}$$

Here, E is the Young's modulus, a is the cross-sectional area, and I is the beam's second moment of inertia. In addition, $\mathbf{K}_a^i$ as the stiffness matrix is expressed as a nonlinear function for the absolute nodal coordinates [18]. The elastic force can be obtained by partially differentiating the total strain energy into generalized coordinates as in Eq. (9), and it changes depending on the time. Therefore, the required calculations outnumber those needed for the mass matrix of Eq. (6).

$$\left(\frac{\partial U^i}{\partial \mathbf{e}^i}\right) = \mathbf{Q}_k^i \tag{9}$$

Until now, the study was illustrated based on the classic Euler-Bernoulli beam theory to calculate the elastic force.

2.2 Dynamic Equation of a Constrained Flexible Beam

The dynamic equation of a constrained flexible beam, which can present a large deformable cable or wire, can be written as Eq. (10) after going through the general assembly process used in the Finite Element Method [19].

$$\mathbf{M}^a\ddot{\mathbf{e}} + \boldsymbol{\Phi}_\mathbf{e}^T\boldsymbol{\lambda} + \mathbf{Q}_k + \mathbf{Q}_d = \mathbf{Q}_e \tag{10}$$

In this equation, $\mathbf{M}^a$ is the assembled global mass matrix of the beam elements and $\boldsymbol{\Phi} = \boldsymbol{\Phi}(\mathbf{e}, t)$ is the constraint equation. $\boldsymbol{\Phi}_\mathbf{e}$ is the constraint Jacobian matrix and $\boldsymbol{\lambda}$ is the Lagrange multiplier vector. $\mathbf{Q}_k$ is the elastic force vector and $\mathbf{Q}_d$ is the structural damping force vector for the flexible beam element. $\mathbf{Q}_e$ is the generalized external force vector caused by gravity and spring-damper element. Here, a linear model of damping force is used to consider internal structural damping effects. In other words, a particular form of the proportional Rayleigh damping method is used in Eq. (11) [20-21].

$$\mathbf{Q}_d = \mathbf{C}\dot{\mathbf{e}}$$
$$\mathbf{C} = \alpha\mathbf{M}^a + \beta\mathbf{K}_a$$
$$\alpha = \frac{2\omega_1\omega_2(\xi_1\omega_2 - \xi_2\omega_1)}{\omega_2^2 - \omega_1^2} \tag{11}$$
$$\beta = \frac{2(\xi_2\omega_2 - \xi_1\omega_1)}{\omega_2^2 - \omega_1^2}$$

Here, $\mathbf{K}_a$ is the assembled stiffness matrix from Eq. (8). The coefficients α and β depend on the frequencies ω_1 and ω_2, as well as on the damping ratios ξ_1 and ξ_2 for the first two modes of the beam. The frequencies ω_1 and ω_2 should be calculated by eigen value analysis using Eq. (10), and the ratios ξ_1 and ξ_2 should be calculated from experimental data [20-21]. When second differentiation was done on time in $\boldsymbol{\Phi}$, the right-hand side of acceleration for the constraint equation [22-23] can be obtained as Eq. (12).

$$\boldsymbol{\Phi}(\mathbf{e}, t) = \mathbf{0}$$
$$\boldsymbol{\Phi}_\mathbf{e}\ddot{\mathbf{e}} = -(\boldsymbol{\Phi}_\mathbf{e}\dot{\mathbf{e}})_\mathbf{e}\dot{\mathbf{e}} - 2\boldsymbol{\Phi}_{\mathbf{e}t}\dot{\mathbf{e}} - \boldsymbol{\Phi}_{tt} = \boldsymbol{\gamma} \tag{12}$$

If Eqs. (10) and (12) are written in matrix form, the dynamic equation of the flexible beam can be obtained using only absolute nodal coordinates as Eq. (13).

$$\begin{bmatrix} \mathbf{M}^a & \boldsymbol{\Phi}_\mathbf{e}^T \\ \boldsymbol{\Phi}_\mathbf{e} & \mathbf{0} \end{bmatrix} \begin{bmatrix} \ddot{\mathbf{e}} \\ \boldsymbol{\lambda} \end{bmatrix} = \begin{bmatrix} \mathbf{Q}^a \\ \boldsymbol{\gamma} \end{bmatrix} \tag{13}$$

Here, $\mathbf{Q}^a = \mathbf{Q}_e - \mathbf{Q}_k - \mathbf{Q}_d$.

3. Combined System Equations of Motion and Dynamic Stress Calculation

3.1 System Equations of Motion Including a Flexible Beam

Up to this point, we only derived the dynamic equations of the large flexible beam using absolute nodal coordinates. To analyze the dynamic interaction with the multibody system, which is a rigid body, after coupling, there should be a system equations of motion that includes various constraint equations between the flexible beam and the multibody system. Consequently, in order to consider both flexible beams and rigid bodies simultaneously in a multibody system, a new generalized coordinate system must be defined, as in the form $\mathbf{q}=[\mathbf{r}^T, \mathbf{e}^T]$. Additionally, in the constraint equation $\mathbf{\Phi}(\mathbf{r},\mathbf{e},t)=\mathbf{0}$, the mass matrix also needs to be redefined. Consequently, the system's equations of motion can be written as Eq. (14).

$$\begin{bmatrix} \mathbf{M}^{\mathrm{r}} & \mathbf{0} & \mathbf{\Phi}_{\mathrm{r}}^T \\ \mathbf{0} & \mathbf{M}^{\mathrm{a}} & \mathbf{\Phi}_{\mathrm{e}}^T \\ \mathbf{\Phi}_{\mathrm{r}} & \mathbf{\Phi}_{\mathrm{e}} & \mathbf{0} \end{bmatrix} \begin{bmatrix} \ddot{\mathbf{r}} \\ \ddot{\mathbf{e}} \\ \boldsymbol{\lambda} \end{bmatrix} = \begin{bmatrix} \mathbf{Q}^{\mathrm{r}} \\ \mathbf{Q}^{\mathrm{a}} \\ \boldsymbol{\gamma} \end{bmatrix} \tag{14}$$

Here, $\mathbf{r}=[\mathbf{r}^1,\mathbf{r}^2,\cdots\mathbf{r}^{\mathrm{nr}}]$ is the rigid body coordinates to define the multibody, where nr is the number of rigid bodies that compose the multibody, and the $\mathbf{r}^{\mathrm{k}}$ vector has three components as $\mathbf{r}^{\mathrm{k}}=[\mathrm{x}^{\mathrm{k}},\mathrm{y}^{\mathrm{k}},\theta^{\mathrm{k}}]^{\mathrm{T}}$. $\mathbf{M}^{\mathrm{r}}$ is the rigid bodies' mass matrix, $\mathbf{\Phi}_{\mathrm{r}}$ is the Jacobian matrix for the rigid body coordinates, and $\mathbf{Q}^{\mathrm{r}}$ is the generalized external force for the rigid body coordinates. Eq. (14) is a differential algebraic equation, and to solve such an equation, many methods are suggested [22-23]. In this study, 4-th Runge-Kutta Integration Method was used to solve Eq. (14).

3.2 Stress Calculation of a Beam Element Using Absolute Nodal Coordinates

When considering Eq. (14), it is possible to calculate the dynamic stresses of a beam in a multibody system, because the equation is derived based on the continuous mechanics theory and the finite element method. The dynamic stress can be used to predict the fatigue life of a mechanical part [16]. This study presents the computation method based on Euler-Bernoulli beam theory.

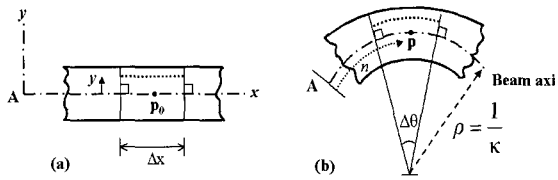

Fig. 3 (a) Undeformed and (b) Deformed beam segment

Fig. 3 shows the arbitrary point at the undeformed and deformed beam segment, which is shown in Fig. 2, where ρ is the curvature radius and the reciprocal of the curvature κ. The bending moment at position $\mathbf{p}$ of the deformed beam can be written in terms of the beam's curvature as follows [24].

$$M = E\,I\,\kappa = \frac{E\,I}{\rho} \tag{15}$$

Here, the curvature κ can be written as Eq. (16) using Serret-Frenet formulas [25].

$$\kappa = \left|\frac{d^2\mathbf{r}}{dn^2}\right| = \frac{|\mathbf{r}'\times\mathbf{r}''|}{|\mathbf{r}'|^3} = \frac{\mathbf{r}''^T\tilde{\mathbf{I}}\mathbf{r}'}{|\mathbf{r}'^T\mathbf{r}'|^{3/2}} = \frac{\mathbf{r}''^T\tilde{\mathbf{I}}\mathbf{r}'}{f^3}$$
$$dn = \sqrt{\mathbf{r}'^T\mathbf{r}'}dx \quad , \quad \mathbf{r}' = \frac{d\mathbf{r}}{dx} \quad , \quad \tilde{\mathbf{I}} = \begin{bmatrix} 0 & -1 \\ 1 & 0 \end{bmatrix} \tag{16}$$
$$f = |\mathbf{r}'^T\mathbf{r}'|^{1/2}$$

Here, n is the length along its curvature. If the deformation in the longitudinal direction is minimal, $f \approx 1$, and Eq. (16) can be written as Eq. (17).

$$\kappa \approx \left|\frac{d^2\mathbf{r}^i(x,t)}{dx^2}\right| = |\mathbf{r}''| = \left|\left[\frac{d^2}{dx^2}\mathbf{S}^i(x)\right]\mathbf{e}^i(t)\right|$$
$$(\mathbf{S}^i)'' = \begin{bmatrix} S_x'' \\ S_y'' \end{bmatrix} = \begin{bmatrix} S_1'' & 0 & S_2'' & 0 & S_3'' & 0 & S_4'' & 0 \\ 0 & S_1'' & 0 & S_2'' & 0 & S_3'' & 0 & S_4'' \end{bmatrix} \tag{17}$$

However, if the longitudinal deformation may not be ignored, the value of f must be considered seriously in

Eq. (16). The strain and stress with respect to time at an arbitrary point of a beam that has undergone bending deformation can be expressed as in Eq. (18) [24].

$$\varepsilon_x(x,y,t) = y\,\kappa(x,t) = \frac{y}{\rho}$$
$$\sigma_x(x,y,t) = E\varepsilon_x = Ey\kappa = \frac{My}{I} \tag{18}$$

If the absolute nodal coordinates $\mathbf{e}^i(t)$ of a beam element that considers the effects of kinetic inertia are calculated from Eq. (14), the beam element's curvature at an arbitrary point can be calculated by Eq. (17). Furthermore, dynamic stress distribution can be predicted by Eq. (18). In order to use this calculated dynamic stress in the fatigue analysis, either the maximum stress must be found, or the stress at the Barlow point [26] may be used. This choice is left to the discretion of the engineer carrying out the fatigue analysis. This presented method is significant in that it brings up the possibility of merging the two fields of multibody dynamics and structural dynamics, and perhaps even additional fatigue analysis, into one numerical model.

3.3 Numerical Example (1): Large Deformation and Stress Analysis of a Flexible Beam

In this study, an analysis program for Eq. (14) including Eq. (17) and Eq. (18) was developed. This was then used to calculate the large displacement and the dynamic stress of a cantilever beam with respect to time. The reliability of this program was compared to the real experimental result in a reference [21] for verification. Fig. 4 shows the simulation model and Table 1 presents the data used in the simulation.

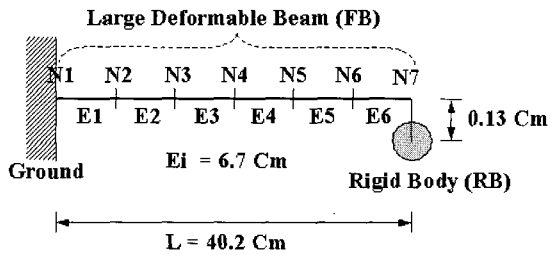

Fig. 4 Simulation model for calculating the large displacement of flexible beam

Table 1 Simulation model data (1)

Body	Data	비 고
FB (Beam)	Total Length: 0.402 M Beam Elements: 6 (Circular Section)	Very Flexible
	Total Mass (kg): 0.0025 Diameter (mm): 1 Cross Area(m^2): 785.4×10^{-9} I (m^4): 4.909×10^{-14} E (GPa): 200.0 $\alpha = 0.02$ $\beta = 0.0$ (not considered)	
RB	Mass (kg): 0.02 Inertia ($kg\,m^2$): 1.58×10^{-6}	Rigid
Ground		Fix

A rigid body was attached at the beams's end-point N7 using a fixed joint. For a more accurate analysis, the beam's structural damping was considered using Eq. (11) Damping coefficient data α, β are same as the reference. In addition, the longitudinal deformation will be ignored, so Eq. (17) may be used. The calculation position of the dynamic stress is at the midpoint of E1 and the surface (y= 0.5mm).

Fig. 5 shows the large deformable behavior of a beam related to time.

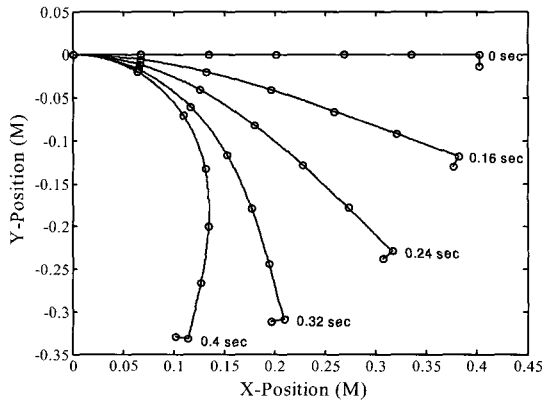

Fig. 5 Large deformation behavior of flexible beam

Fig. 6 shows the changes of Y-direction displacement of node N7, compared with the results by the experiment and the commercial FEA program NASTRAN (Nonlinear Transient Response Analysis [15]). As shown in the figure, the analysis result by the presented method is very similar to the experiment data.

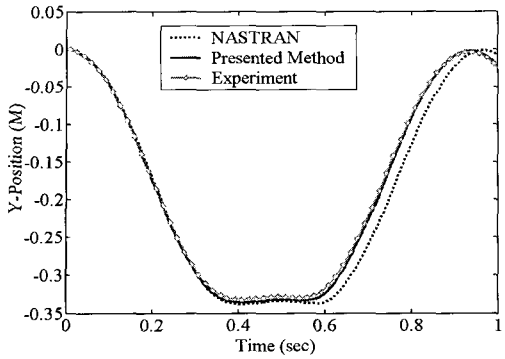

Fig. 6 Analysis result of large displacement

Fig. 7 shows the analysis results of dynamic stress by the presented method and NASTRAN. As shown in the figure, the maximum stresses were similar, but there was a slight difference in phase and magnitude. This may be the result of a difference in displacement. And we assumed that this was caused by the characteristics of the time increment method or element properties used in NASTRAN.

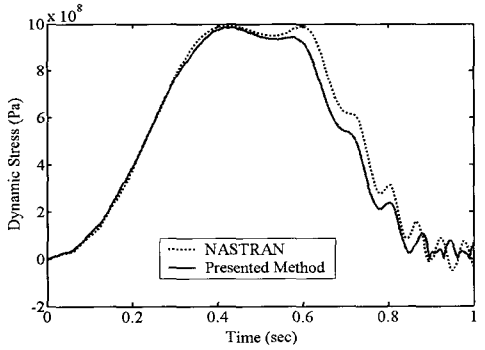

Fig. 7 Analysis result of dynamic stress

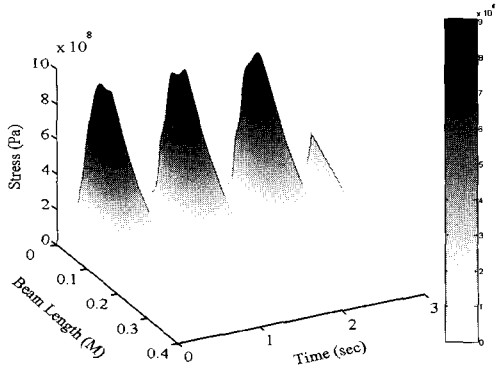

Fig. 8 Stress distribution along beam length depending on time

Fig. 8 shows the dynamic stress distribution along its length depending on time when 6 beam elements are used in presented method.

This study may be applied to improve the reliability of many mechanical systems, such as robot's electric harness and very flexible space structures, by calculating the dynamic stress during multibody dynamic simulation.

4. System Equations of Motion Including Sliding Constraints

In this chapter, we derived the generalized system dynamic equations of motion that can analyze a more complex system which includes a constraint equation for the sliding joint between a large deformable beam and a rigid multibody. Using this equation, we can simultaneously analyze the behaviors of a large fleixble cable and a multibody system.

4.1 Constraint Equations of a Sliding Joint

Fig. 9 shows the concept of the sliding joint when the multibody system, which is a rigid body, moves along a flexible cable, and to model this, a non-generalized coordinate n is introduced. The non-generalized coordinate is in a coordinate system that does not relate to mass and external force.

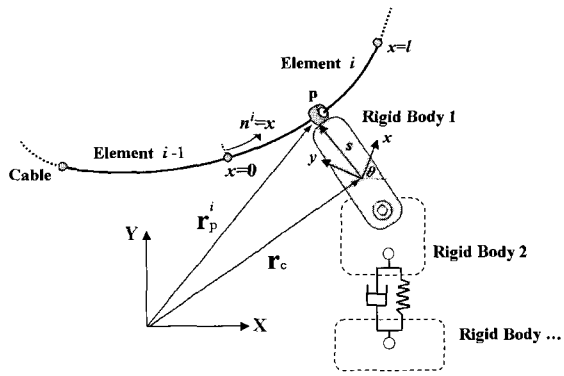

Fig. 9 Multibody system moving along a cable

The constraint equation of the sliding joint can be defined as Eq. (19) using Eq. (1). In other words, the constraint equation can be defined by making the position of point **p**, which was defined using rigid body coordinates (x-y), the same as the absolute position defined from the arbitrary beam elements that compose the cable.

$$\begin{aligned}\boldsymbol{\Phi}(\mathbf{r},\mathbf{e},n,t) &= \mathbf{r}_{\mathrm{p}}^{i} - \mathbf{r}^{\mathrm{R}} = \mathbf{0} \\ &= \mathbf{S}^{i}(x=n)\,\mathbf{e}^{i}(t) - \mathbf{r}^{\mathrm{R}} = \mathbf{0}\end{aligned} \tag{19}$$

Here, $\mathbf{r}^{\mathrm{R}} = [\mathbf{r}_x^{\mathrm{R}}, \mathbf{r}_y^{\mathrm{R}}]^T = \mathbf{r}_{\mathrm{c}} + \mathbf{A}\mathbf{s}$ and $\mathbf{A}$ is the transformation matrix of the rigid body reference frame (x-y) for the global reference frame (X-Y). $\mathbf{s} = [\mathbf{s}_x, \mathbf{s}_y]$ is the displacement of the point $\mathbf{p}$ defined from the rigid body reference frame, and it is always constant. $\mathbf{r}_{\mathrm{p}}^{i}$ is the global displacement of the p point defined from the beam element i, and it changes depending on the non-generalized coordinate n.

When $\mathbf{r}_{\mathrm{p}}^{i}$ does not change due to the constant value of n in Eq. (19), it becomes a constraint equation for the fixed joint that can define the knot of the multibody system and cable. When Eq. (19) is extended, it can be expressed as two constraint equations for x and y directions as Eq. (20).

$$\begin{aligned}\boldsymbol{\Phi}^{i(x)} = {} & \mathbf{e}_1^i\left(1-\frac{3n^2}{l^2}+\frac{2n^2}{l^3}\right)+\mathbf{e}_3^i\left(n-\frac{2n^2}{l}+\frac{n^3}{l^2}\right) \\ & +\mathbf{e}_5^i\left(\frac{3n^2}{l^2}-\frac{2n^3}{l^3}\right)\quad+\mathbf{e}_7^i\left(-\frac{n^2}{l}+\frac{n^3}{l^2}\right) \\ & -\mathbf{r}_x^{\mathrm{R}} = 0 \\ \boldsymbol{\Phi}^{i(y)} = {} & \mathbf{e}_2^i\left(1-\frac{3n^2}{l^2}+\frac{2n^2}{l^3}\right)+\mathbf{e}_4^i\left(n-\frac{2n^2}{l}+\frac{n^3}{l^2}\right) \\ & +\mathbf{e}_6^i\left(\frac{3n^2}{l^2}-\frac{2n^3}{l^3}\right)\quad+\mathbf{e}_8^i\left(-\frac{n^2}{l}+\frac{n^3}{l^2}\right) \\ & -\mathbf{r}_y^{\mathrm{R}} = 0\end{aligned} \tag{20}$$

Using the constraint equation coupled on the rigid body coordinates and absolute nodal coordinates of Eq. (20), the Jacobian matrix and the right-hand side of acceleration of the sliding joint can be calculated. The calculation results are arranged in the appendix. The friction on the sliding joint was not considered in this study.

4.2 System Equations of Motion Including Sliding Constraints

To consider the dynamic interaction between a rigid multibody and a flexible cable, a new system coordinates $\mathbf{q} = [\mathbf{r}^T, \mathbf{e}^T, n]^T$ is introduced that include both the rigid body coordinates and the nongeneralized coordiante which are used, respectively, to define the multibody system and the sliding joint. Therefore, the constraint equation of Eq. (12) becomes $\boldsymbol{\Phi}(\mathbf{r},\mathbf{e},n,t) = \mathbf{0}$ and it includes the constraint equation of the sliding joint to implement the dynamic interaction of the multibody system and the flexible beam. The mass matrix is redefined, so Eq. (14) can be used as the final equations for the analysis of the interaction of the flexible beam and the multibody system as Eq. (21).

$$\begin{bmatrix} \mathbf{M}^r & \mathbf{0} & \mathbf{0} & \boldsymbol{\Phi}_{\mathbf{r}}^T \\ \mathbf{0} & \mathbf{M}^a & \mathbf{0} & \boldsymbol{\Phi}_{\mathbf{e}}^T \\ \mathbf{0} & \mathbf{0} & 0 & \boldsymbol{\Phi}_n^T \\ \boldsymbol{\Phi}_{\mathbf{r}} & \boldsymbol{\Phi}_{\mathbf{e}} & \boldsymbol{\Phi}_n & 0 \end{bmatrix} \begin{bmatrix} \ddot{\mathbf{r}} \\ \ddot{\mathbf{e}} \\ \ddot{n} \\ \boldsymbol{\lambda} \end{bmatrix} = \begin{bmatrix} \mathbf{Q}^r \\ \mathbf{Q}^a \\ 0 \\ \boldsymbol{\gamma} \end{bmatrix} \tag{21}$$

Here, $\boldsymbol{\Phi}_n$ is the Jacobian matrix for the non-generalized coordinate. Eq. (21) is also a differential algebraic equation.

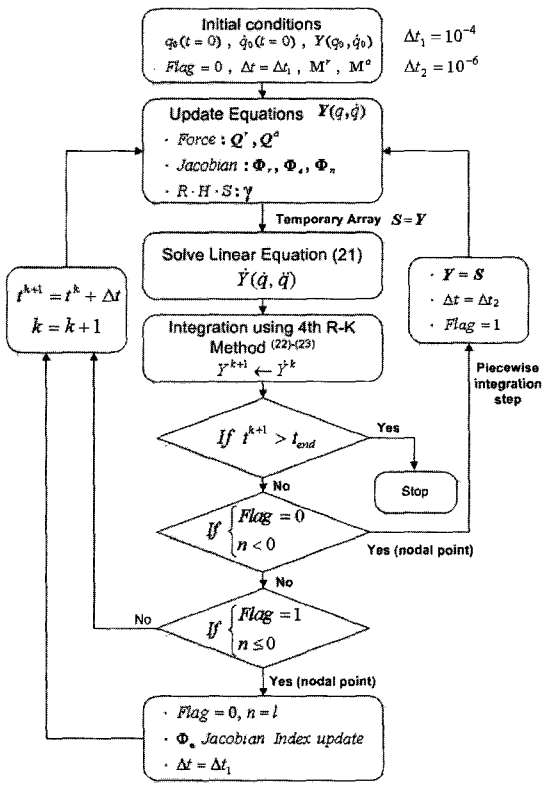

Fig. 10 Numerical algorithm

Fig. 10 shows the concept that allows the connection point (nodal point) to avoid the discontinuouity problem by reconstructing the Jacobian matrix when the sliding joint moves from element i to element i-1. For this, there should be an algorithm that can determine the moment when the integrator for the analysis of Eq. (21) passes the nodal point. Using the integration method of 4-th Runge-Kutta, the study determined the beam element i-1 where the sliding joint moves in the integration step where $n^i \leq 0$, and developed a program that can advance the analysis of the system by reconstructing the Jacobian matrix for the generalized coordinates of the beam element.

4.3 Numerical Example (2): Analysis of a Flexible Catenary Cable Carrying a Moving Multibody System

Fig. 11 shows a model for the numerical example of this study. Table 2 shows the material properties of the cable and multibody system.

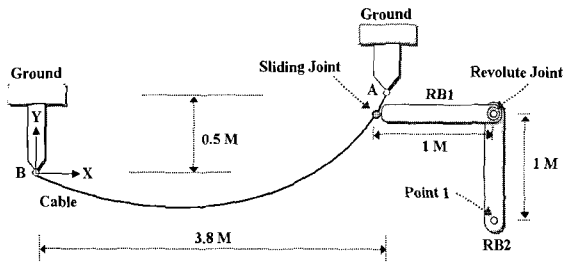

Fig. 11 Simulation model

Table 2 Simulation model data (2)

Body	Data	비고
Cable	Total Length: 4.02 M Beam Elements: 12, 18, 24 (Circular Section)	Very Flexible
	Total Mass (kg): 0.148 Diameter (mm): 3 CrossArea (m^2): 7.068×10^{-6} I (m^4): 7.952×10^{-12} E (GPa): 200.0 $\alpha = 0.01$ $\beta = 0.0$ (not considered)	
RB1 RB2	Mass (kg): 2.67 Inertia ($kg \cdot m^2$): 0.2242	Rigid

The cable was modeled using 12, 18, and 24 beam elements, respectively, and each model was analyzed. The values of structural damping coefficient α, and β are assumed by the reference [21].

Fig. 12 shows the behavior of the cable and multibody when the simulation was executed using 24 beam elements in the model. As shown in this result, the large deformation phenomenon of the cable was well realized by the presented method.

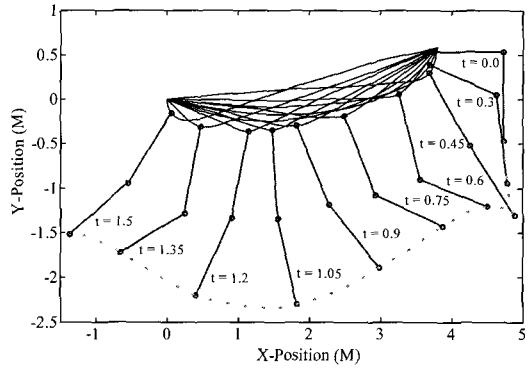

Fig. 12 Behaviors of cable and multibody

Fig. 13 shows the path of point 1 where the number of beam elements that compose the cable was modified. In the case of using 12 beam elements, it was insufficient to present the large deformable motion of the cable, where the sliding joint was located in the largest deformable area (approximately, after 1.3sec). However, in using more than 18 beam elements, we concluded that it was adequate to analyze the large deformable behavior of the cable.

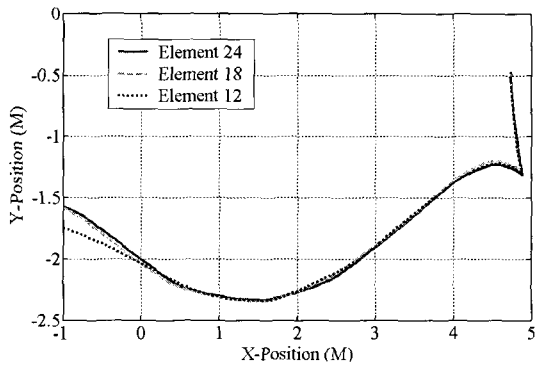

Fig. 13 Trajectory of point 1

In cable problem, if the dynamic stress is calculated by Eq. (18), the value f in Eq. (16) must be calculated in consideration to the longitudinal deformation.

5. Conclusions

In this paper, the equations of motion that can analyze the dynamic interaction of a very flexible beam and a multibody system were derived. Using the derived equations, a method for calculating the dynamic stress of a large deformable beam was proposed, and its reliability was verified through comparison with the results from experiments and the commercial program NASTRAN. This is significant in that it brings up the possibility of merging the two fields of multibody dynamics and structural dynamics, and perhaps even additional fatigue analysis, into one numerical model.

In addition, the study developed a sliding joint where the multibody system can move along the very flexible cable. In the future, there should be studies that consider friction and the development of a driver that can operate the sliding joint under the constraint condition of time. In addition, the methods of the study should be applied to an actual system, and their efficiency and reliability need to be verified through real experiments.

This study can be applied to various multibody systems that include large deformable problems of beams, which were hard to analyze. In other words, it can be applied to actual mechanical fields such as ski lifts, cable cars, the pantograph and catenary of high-speed trains, pulley systems, and marine hoist cables.

References

1. Valembois, R. E., Fisette, P. and Samin, J. C., "Comparison of Various Techniques for Modeling Flexible Beams in Multibody Dynamics," Journal of Nonlinear Dynamics, Vol. 12, pp. 367-397, 1997.
2. Huston, R. L. and Passerello, C. E., "Validation of Finite Segment Cable Models," Journal of Computers and Structures, Vol. 15, No. 6, pp. 653-660, 1982.
3. Winget, J. M. and Huston, R. L., Cable Dynamics -A finite Segment Approach, Journal of Computers and Structures, Vol. 6, pp. 475-480, 1976.
4. Kamman, J. W. and Huston, R. L., "Multibody Dynamics Modeling of Variable Length Cable Systems," Journal of Multibody System Dynamics, Vol. 5, pp. 211-221, 2001.
5. Hwang, R. S. and Haug, E. J., "Translational Joints in Flexible Multibody Dynamics," Journal of Mechanical Structures and Machines, Vol. 18, No. 4, pp. 543-564, 1990.
6. Park, C. J. and Park, T. W., "Dynamic Analysis of a Moving Vehicle on Flexible Beam Structures," International Journal of the Korean Society of Precision Engineering, Vol. 3, No. 4, pp. 54-71, 2002.
7. Sugiyama, H., Escalona, J. and Shabana, A. A., "Formulation of Three-dimensional Joint Constraints Using Absolute Nodal Coordinates," Journal of Nonlinear Dynamics, Vol. 31, pp. 167-195, 2003.
8. Simo, J. C. and Vu-Quoc, L., "On The Dynamics of Flexible Beams under Large Overall Motions-The Plane Case: Part 1 and Part 2," ASME International Journal of Applied Mechanics, Vol. 53, No. 4, pp. 849-863, 1986.
9. Sharf, I., "Geometrically Nonlinear Beam Element for Dynamics Simulation of Multibody Systems," Journal of Numerical Methods in Engineering, Vol. 39, pp. 763-786, 1996.
10. Yoshimura, T., Hino, J. and Kamata, T., "Random Vibration of a Non-linear Beam Subjected to Moving Load: A Finite Element Method Analysis," Journal of Sound and Vibration, Vol. 122, No. 2, pp. 317-329, 1988.
11. Lee, H. P., "The Dynamic Response of a Timoshenko Beam Subjected to a Moving Mass," Journal of Sound and Vibration, Vol. 198, No. 2, pp. 249-256, 1996.
12. Mayo, J., Domingues, J. and Shabana, A. A., "Geometrically Nonlinear Formulations of Beams in Flexible Multibody Dynamics," Journal of Vibration and Acoustics, Vol. 117, pp. 501-509, 1995.
13. Shabana, A. A., "Computer Implementation of The Absolute Nodal Coordinates Formulation for Flexible Multibody Dynamics," Journal of Nonlinear Dynamics, Vol. 16, pp. 293-306, 1998.
14. Escalona, J. L. and Hussien, H. A., "Application of The Absolute Nodal Coordinates Formulation to Multibody System Dynamics," Journal of Nonlinear Dynamics, Vol. 16, pp. 293-306, 1998.
15. MSC/NASTRAN Manual, The Macneal-Schwendler Corporation, 1996.

16. Liu, T. S. and Haug, E. J., "Computational Methods for Life Prediction of Mechanical Components of Dynamic System," Technical Report 86-24, CADSI, The University of IOWA, 1986.
17. Shabana, A. A., Dynamics of Multibody Systems, Cambridge University Press, pp. 311-323, 1998.
18. Berzeri, M. and Shabana, A. A., "Development of Simple Models for The Elastic Forces in The Absolute Nodal Coordinate Formulation," Journal of Sound and Vibration, Vol. 235, No. 4, pp. 539-565, 2000.
19. Huebner, K. H., The finite element method for engineers, John Wiley & Sons, pp. 38-54, 1995.
20. Takahashi, Y., Shimizu, N. and Suzuki, K., "Introduction of Damping Matrix into Absolute Nodal Coordinate Formulation," Proceedings of The First Asian Conference on Multibody Dynamics (ACMD' 2002), pp. 33-40, 2002.
21. Yoo, W. S., Lee, S. J. and Sohn, J. H., "Physical Experiments for Large Deformation Problems," Proc. of the KSME Spring Conference, No. 03S115, pp. 705-710, 2003.
22. Haug, E. J., Computer-Aided Kinematics and Dynamics of Mechanical Systems, Allyn and Bacon, 1989.
23. Nikravesh, P. E., Computer-Aided Analysis of Mechanical System, Prentice-Hall, 1988.
24. Craig R. R., Mechanics of Materials, John Wiley & Sons, pp. 258-265, 1996.
25. Goetz, A., Introduction to Differential Geometry, Addison Wesley Company, 1970.
26. Barlow, J., "Optimal Stress Locations in Finite Element Models," Journal of Numerical Methods in Engineering, Vol. 10, pp. 243-251, 1976.

APPENDIX

A.1 Jacobian Matrix for a Sliding Joint

$$\underbrace{x_1\ y_1\ \theta_1}_{\Phi_r^i}\ \cdots\ \underbrace{e_1^i\ e_2^i\ e_3^i\ e_4^i\ e_5^i\ e_6^i\ e_7^i\ e_8^i}_{\Phi_e^i}\ \cdots\ \underbrace{n}_{\Phi_n^i}$$

$$\Phi_q^i = \begin{bmatrix} \Phi_q^{i(x)} \\ \Phi_q^{i(y)} \end{bmatrix} = \begin{bmatrix} 1 & 0 & \mathbf{A}_1 & \cdots & s_1 & 0 & s_2 & 0 & s_3 & 0 & s_4 & 0 & \cdots & \mathbf{A}_2 \\ 0 & 1 & \mathbf{B}_1 & \cdots & 0 & s_1 & 0 & s_2 & 0 & s_3 & 0 & s_4 & \cdots & \mathbf{B}_2 \end{bmatrix}$$

Here,

$$S_1 = 1 - \frac{3n^2}{l^2} + \frac{2n^3}{l^3}\ ,\quad S_2 = n - \frac{2n^2}{l} + \frac{n^3}{l^2}$$

$$S_3 = \frac{3n^2}{l^2} - \frac{2n^3}{l^3}\ ,\quad S_4 = -\frac{n^2}{l} + \frac{n^3}{l^2}$$

$$\mathbf{A}_1 = \mathbf{s}_x\dot{\theta}\sin\theta + \mathbf{s}_y\dot{\theta}\cos\theta\ ,\quad \mathbf{B}_1 = -\mathbf{s}_x\dot{\theta}\cos\theta + \mathbf{s}_y\dot{\theta}\sin\theta$$

$$\mathbf{A}_2 = e_1^i\left(-\frac{6n}{l^2}+\frac{6n^2}{l^3}\right) + e_3^i\left(1-\frac{4n}{l}+\frac{3n^2}{l^2}\right) + e_5^i\left(\frac{6n}{l^2}-\frac{6n^2}{l^3}\right) + e_7^i\left(-\frac{2n}{l}+\frac{3n^2}{l^2}\right)$$

$$\mathbf{B}_2 = e_2^i\left(-\frac{6n}{l^2}+\frac{6n^2}{l^3}\right) + e_4^i\left(1-\frac{4n}{l}+\frac{3n^2}{l^2}\right) + e_6^i\left(\frac{6n}{l^2}-\frac{6n^2}{l^3}\right) + e_8^i\left(-\frac{2n}{l}+\frac{3n^2}{l^2}\right)$$

A.2 Right Hand Side of Acceleration for a Sliding Joint

$$\Phi_q^i\ddot{\mathbf{q}} = \begin{bmatrix} \Phi_q^{i(x)}\ddot{\mathbf{q}} \\ \Phi_q^{i(y)}\ddot{\mathbf{q}} \end{bmatrix}$$

$$= \begin{bmatrix} (\mathbf{s}_x\cos\theta - \mathbf{s}_y\sin\theta)\dot{\theta}^2 \\ \quad + 2\dot{n}[\dot{e}_1^i\left(-\frac{6n}{l^2}+\frac{6n^2}{l^3}\right) + \dot{e}_3^i\left(1-\frac{4n}{l}+\frac{3n^2}{l^2}\right) + \dot{e}_5^i\left(\frac{6n}{l^2}-\frac{6n^2}{l^3}\right) + \dot{e}_7^i\left(-\frac{2n}{l}+\frac{3n^2}{l^2}\right)] \\ \quad + \ddot{n}^2\left[e_1^i\left(-\frac{6}{l^2}+\frac{12n}{l^3}\right) + e_3^i\left(-\frac{4}{l}+\frac{6n}{l^2}\right) + e_5^i\left(\frac{6}{l^2}-\frac{12n}{l^3}\right) + e_7^i\left(-\frac{2}{l}+\frac{6n}{l^2}\right)\right] \\ \\ (\mathbf{s}_x\sin\theta + \mathbf{s}_y\cos\theta)\dot{\theta}^2 \\ \quad + 2\dot{n}[\dot{e}_2^i\left(-\frac{6n}{l^2}+\frac{6n^2}{l^3}\right) + \dot{e}_4^i\left(1-\frac{4n}{l}+\frac{3n^2}{l^2}\right) + \dot{e}_6^i\left(\frac{6n}{l^2}-\frac{6n^2}{l^3}\right) + \dot{e}_8^i\left(-\frac{2n}{l}+\frac{3n^2}{l^2}\right)] \\ \quad + \ddot{n}^2\left[e_2^i\left(-\frac{6}{l^2}+\frac{12n}{l^3}\right) + e_4^i\left(-\frac{4}{l}+\frac{6n}{l^2}\right) + e_6^i\left(\frac{6}{l^2}-\frac{12n}{l^3}\right) + e_8^i\left(-\frac{2}{l}+\frac{6n}{l^2}\right)\right] \end{bmatrix}$$